separations

MDPI

Article

Inhibitory Effect and Mechanism of Dill Seed Essential Oil on *Neofusicoccum parvum* in Chinese Chestnut

Tian-Tian Liu [1,2], Lin-Jing Gou [1,2], Hong Zeng [3], Gao Zhou [1,2], Wan-Rong Dong [1], Yu Cui [1], Qiang Cai [4,*] and Yu-Xin Chen [1,2,*]

1 Hubei Key Laboratory of Industrial Microbiology, Key Laboratory of Fermentation Engineering (Ministry of Education), Cooperative Innovation Center of Industrial Fermentation (Ministry of Education & Hubei Province), Hubei University of Technology, Wuhan 430068, China
2 National "111" Center for Cellular Regulation and Molecular Pharmaceutics, School of Food and Biological Engineering, Hubei University of Technology, Wuhan 430068, China
3 Xinjiang Production & Construction Corps, Key Laboratory of Protection and Utilization of Biological Resources in Tarim Basin, College of Life Sciences, Tarim University, Alaer 843300, China
4 Department of Plant Science, School of Life Sciences, Wuhan University, Wuhan 430072, China
* Correspondence: qiang.cai@whu.edu.cn (Q.C.); yuxinc@hbut.edu.cn (Y.-X.C.)

Abstract: The chestnut postharvest pathogen *Neofusicoccum* parvum (*N. parvum*) is an important postharvest pathogen that causes chestnut rot. Chestnut rot in postharvest reduces food quality and causes huge economic losses. This study aimed to evaluate the inhibitory effect of dill seed essential oil (DSEO) on *N. parvum* and its mechanism of action. The chemical characterization of DSEO by gas chromatography/mass spectrometry (GC/MS) showed that the main components of DSEO were apiole, carvone, dihydrocarvone, and limonene. DSEO inhibited the growth of mycelium in a dose-dependent manner. The antifungal effects are associated with destroying the fungal cell wall (cytoskeleton) and cell membrane. In addition, DSEO can induce oxidative damage and intracellular redox imbalance to damage cell function. Transcriptomics analysis showed DSEO treatment induced differently expressed genes most related to replication, transcription, translation, and lipid, DNA metabolic process. Furthermore, in vivo experiments showed that DSEO and DSEO emulsion can inhibit the growth of fungi and prolong the storage period of chestnuts. These results suggest that DSEO can be used as a potential antifungal preservative in food storage.

Keywords: dill; *Anethum graveolens* L.; essential oil; *Neofusicoccum parvum*; antifungal mechanism

Citation: Liu, T.-T.; Gou, L.-J.; Zeng, H.; Zhou, G.; Dong, W.-R.; Cui, Y.; Cai, Q.; Chen, Y.-X. Inhibitory Effect and Mechanism of Dill Seed Essential Oil on *Neofusicoccum parvum* in Chinese Chestnut. *Separations* **2022**, *9*, 296. https://doi.org/10.3390/separations9100296

Academic Editor: Xingchu Gong

Received: 17 September 2022
Accepted: 7 October 2022
Published: 9 October 2022

1. Introduction

Chestnuts (Castanea) belonging to the family Fagaceae are distributed mainly in eastern Asia, southwestern Asia, southern Europe, and North America [1]. The world's economic cultivation of chestnut plants includes mainly the Chinese chestnut (*Castanea mollissima* Bl.), Japanese chestnut (*C. crenata* Si.), and European chestnut (*C. sativa* Mill). As the origin of chestnut, China has a history of planting for more than 3000 years [2]. Chestnut is an important food resource, which is rich in nutritional value and has the laudatory name of "king of a thousand fruits". Chestnuts have considerable potential as functional food or food ingredients [1].

Nut rot during storage is a severe problem for chestnuts, which not only causes serious economic losses to the industry but also reduces the supply of nutrients and deteriorates food quality, affecting human health [3]. Italian researchers isolated *Neofusicoccum parvum* (family Botryosphaeriaceae) for the first time from a rot-affected chestnut and showed *N. parvum* caused dark necrosis of the kernel, which is congruent with the nut rot symptoms that occurred in nature [4]. It has been shown that *N. parvum* is one of three major pathogens causing chestnut rot during the chestnut harvest [5]. In addition to chestnut, *N. parvum* has a wide variety of hosts, such as woody plants *Eucalyptus* spp., Pear (*Pyrus* spp.), *Citrus*

limon, and grapes (*Vitis vinifera*), and it has become a growing threat to agricultural and forest ecosystems [4,5]. There is currently no fungicide-specific control *N. parvum*-caused disease of plants. Broad-spectrum fungicides, such as carbendazim and flusilazole, have been used globally. However, it is wildly concerned that the long term use of fungicides causes fungal resistance, environmental pollution, and increasing human health risks [6]. It is worth mentioning that rotten nuts may appear healthy on the outside and are hard to be spotted. Thus, it is required to the development of effective strategies against chestnut rot to ensure that consumers buy good quality nuts. Plant essential oils have been widely used in food preservation and storage and are currently considered new and effective antimicrobial agents.

Dill (*Anethum graveolens* L.) is an annual aromatic herb belonging to the family Umbelliferae. Dill is a traditional spice chopped into soups, lettuce salads, and seafood to enhance the flavor of dishes. Dill seeds are also a traditional spice used primarily in the pickling industry due to their strong smell, such as pickled cucumbers, which can be eaten to repel insects [7,8]. Dill seed essential oil (DSEO) is a potent inhibitor of fungal growth, including *Aspergillus flavus*, *Aspergillus niger*, *Fusarium* sp., and *Alternaria alternata* [9,10]. Studies have confirmed that DSEO can be used in the storage and preservation of several foods, such as chickpea food seed, mayonnaise, and corn [9,11,12]. Although extensive investigations have been carried out to study its effective application, there is no consistent finding concerning the DSEO against *N. parvum* in chestnuts. Accordingly, this study aims to determine the inhibitory effect and mechanism of action of DSEO on *N. parvum*. The reliable contact method, liquid shaker method, and gas diffusion method were used to study the inhibitory effect of DSEO on *N. parvum* in vitro. In addition, the effect of DSEO on the fungal cell wall, cell membrane, and oxidative stress were also explored. At the same time, the molecular mechanism of the antifungal activity of DSEO was explored by transcriptomic analysis. Finally, we evaluated the efficacy of DSEO as an antifungal agent in chestnut storage and further expanded the practical application of DSEO in food storage.

2. Materials and Methods

2.1. Plant Materials and Fungal Pathogens

Dill seeds were purchased from the Chinese herbal medicine market in Hotan, Xinjiang Uyghur Autonomous Region of China, and identified by Dr. Gao Zhou. The sample's voucher specimen (No. HM-2020-001) is kept in the Natural Products and Chemical Drug Research and Manufacturing Laboratory, School of Bioengineering and Food, Hubei University of Technology. The mature fruits of chestnut were harvested in Yutoushan Village, Yantianhe Town, Macheng City, Hubei Province. The *N. parvum* used in this study was isolated from rotten chestnut fruit and identified by morphological and molecular biology methods by Dr. Gao Zhou.

2.2. Extraction and Characterization of DSEO

Dried dill seeds (200 g) were smashed, and the EO was obtained via hydrodistillation in 1000 mL H_2O for 5 h using a Clevenger apparatus [7]. After that, the DSEO was kept at 4 °C for further experiments. The chemical characterization of DSEO was performed by gas chromatography/mass spectrometry (GC/MS) [13]. After filtering the sample, 1 µL of the sample was injected into a GC/MS system (Agilent 7890/5975, Agilent Technologies, Santa Clara, CA, USA) and separated on an HP-5ms column (30 m × 0.25 mm × 0.25 µm) (Agilent Technologies). Helium was used as the carrier gas set up at a flow of 1 mL/min. The GC oven temperature increased from 80 °C to 180 °C at a rate of 5 °C/min, and then increased to 260 °C at a 10 °C/min rate. The inlet, interface, ion source, and quadrupole temperatures were set at 250 °C, 250 °C, 230 °C, and 150 °C, respectively. MS data were acquired at a mass range of 20–500 in full scan mode and a solvent delay of 2.5 min. Then, the linear retention index's corresponding relationship was calculated using a mixture of C8-C30 n-alkane (Shanghai Yuanye Biotechnology Co., Ltd., Shanghai, China) according to the Van den Dool and Kratz formula. Essential oil compounds were identified by comparing their

mass spectra with those provided by the National Institute of Standards and Technology (NIST17) database.

2.3. Effect of DSEO on Mycelial Growth

Direct contact assays were used to determine the effect of DSEO on the mycelial growth of *N. parvum* by a previously published method [14]. DSEO was added to PDA to obtain different final concentrations (0.2, 0.4, 0.6, 0.8, and 1 μL/mL). After pouring PDA with or without DSEO into sterilized Petri dishes, the *N. parvum* mycelia blocks (5 mm in diameter) were introduced at the center of the Petri dishes and incubated at 28 ± 2 °C for 4 days.

To inhibit *N. parvum* by vapor contact assays, sterile filter papers with different concentrations of DSEO were placed on the medium-free side of Petri dishes to obtain specific concentrations of DSEO in the air. The mycelia blocks were sealed with parafilm on one side of the medium to prevent vapor leakage from DSEO [15]. The formula for calculating the concentration of DSEO in Petri dishes is as follows:

$$C = V1/V2.$$

V1: Volume of DSEO in filter paper; V2: Volume of Petri dishes.

2.4. Effect of DSEO on Fungal Biomass

Different concentrations of DSEO solution (0, 0.2, 0.4, 0.6, 0.8, 1 μL/mL) were aseptically obtained by diluting DSEO dissolved in 0.1% Tween 20 in a final volume of 25 mL of potato dextrose broth (PDB). Then, the *N. parvum* mycelial block was added to each DSEO solution and incubated in a shaker at 200 r/min at 28 ± 2 °C. After culturing for 3 days, the mycelia were filtered, dried, and weighed [16].

2.5. SEM Observation of the Effect of DSEO on Mycelial Morphology

Studies on the microstructure of mycelia were conducted following a previously described procedure [17]. The *N. parvum* mycelial block was cultured in a PDB medium containing 0.8 μL/mL DSEO (minimum inhibitory concentration) for 3 h. The sample without DSEO treatment acted as a control. All samples were fixed with 2.0% *v*/*v* glutaraldehyde for 24 h at 4 °C and then washed with 100 mM phosphate buffer (pH = 7.4). The samples were then dehydrated with different concentrations (30, 50, 70, 80, 90, 100%) of ethanol. Fixed samples were critical points dried under carbon dioxide and sputter-coated with gold. Then, the changes in mycelium were observed under a scanning electron microscope (SEM) (S-3400, Hitachi, Tokyo, Japan) [15].

2.6. Effect of DSEO on the Cell Wall Integrity

According to the research, the *N. parvum* mycelia suspension was stained with calcofluor white (CFW) [18,19]. After culturing the mycelial suspension for 12 h, DSEO solutions of different concentrations were added to final concentrations of 0.1, 0.2, and 0.4 μL/mL. The culture was continued for 3 h, and 1 mL of mycelial suspension was centrifuged at 6000 rpm for 10 min to remove the culture medium. The collected mycelia samples were stained with 40 μL of CFW and 40 μL KOH (10%). Then, samples were examined using a confocal laser scanning microscope (CLSM) (Leica TCS SP8 CARS). The fungal culture in PDB without DSEO was used as a control.

2.7. Determination of Cellulase Activity

Briefly, the *N. parvum* mycelial block was cultured in blank PDB for 2 days. DSEO solutions of different concentrations were added to final concentrations of 0.2, 0.4, and 0.8 μL/mL, and the culture was continued for 3 h. The sample without DSEO treatment acted as a control. The cellulase activity in *N. parvum* was determined using the 3,5-dinitrosalicylic acid (DNS) colorimetric method [20]. The unit of enzyme activity is defined as follows: the amount of enzyme required to catalyze the production of reducing

sugar equivalent to 1 μg of glucose per hour is determined as 1 unit of enzyme activity, expressed in U/mL. The calculation formula of cellulase enzyme activity is as follows:

$$X\ (U/mL) = (W \times 1000 \times n)/(C \times 180 \times t)$$

W: glucose content in the sample; n: dilution multiple of the sample; C: sample amount; 180: glucose molecular weight; t: reaction time.

2.8. Effect of DSEO Coating on the Membrane Integrity

Evans blue staining was used to prove the cell membrane damage caused by the DSEO treatments [21]. The sample processing is the same as in Section 2.6. Mycelia treated with or without DSEO were stained with Evans blue for 5 min. The mycelia were washed with phosphate-buffered saline (PBS) to remove excess dye. Finally, the mycelia were observed under a microscope (Olympus CX23, Beijing, China) to monitor the membrane integrity of *N. parvum*.

2.9. Determination of Ergosterol Content

Hu et al. and Kong et al. described the spectrophotometric determination of ergosterol content [22,23]. A fungal culture is the same as in Section 2.7. The mycelium was collected by filtration, washed 3 times with distilled water, and filter paper was used to absorb the excess water. An amount of 0.5 g of mycelium was weighed and added to 5 ml of 25% alcoholic potassium hydroxide solution, vibrated vigorously for 10 min, and then incubated at 85 °C for 4 h. A mixture of sterile distilled water and n-heptane (1:3) was used to extract sterols. After vortexing for 10 min, the mixture was allowed to stand for about half an hour to collect the n-heptane layer, which was scanned between 230 and 300 nm by ultraviolet spectrophotometer to determine the sterol amount. The calculated formulas of the ergosterol amount are as follows:

$$(\%)/\text{dehydroergosterol} = (A230/E\ \text{dehydroergosterol})/\text{net wet weight of mycelia}$$

$$(\%)/\text{ergosterol} = (A282/E\ \text{ergosterol})/\text{net wet weight of mycelia} - (\%)/\text{dehydroergosterol}$$

The E value refers to the absorbance of a sample at a specific wavelength through a 1 cm optical path. Among these compounds, E dehydroergosterol = 518, E ergosterol = 90.

2.10. Assessment of Oxidative Stress in N. parvum

A fungal culture is the same as in Section 2.7. The mycelia were collected by filtration and rinsed with distilled water. After the filter paper absorbed excess water, the mycelia were homogenized in an ice bath with different solvents. To determine thiobarbituric acid reactive substances (TBARS), the mycelium was homogenized with 10 times the volume of 10% trichloroacetic acid (TCA) on ice with a glass homogenizer. After centrifuging at 10,000 rpm at 4 °C for 10 min, the supernatant was incubated with 0.67% TCA (1:1) at 95 °C for 30 min, then cooled to room temperature. The reaction product was centrifuged, as described above, and the supernatant was detected at 532 and 600 nm. The TBARS content was expressed as a nmol/mg plot [24]. Superoxide dismutase (SOD) activity and reduced glutathione (GSH) levels were measured using specific kits (Nanjing Jiancheng Bioengineering Institute, Nanjing, China).

2.11. RNA-Sequencing

The mycelia of *N. parvum* cultured for 2 days were exposed to 0.8 μL/mL DSEO, and samples were collected at 1, 2, and 3 h for transcriptome sequencing. The obtained fungal pellets were immediately stored in the liquid nitrogen. All experiments were performed in triplicate, and samples treated without DSEO were used as controls. Total RNA was extracted by TRIzol reagent. The cDNA library construction, RNA-Seq, and the

following analysis were performed by Beijing Novogene Bio-Information Technology Co., Ltd. (Beijing, China).

An amount of 1 μg of RNA in each sample was used to prepare subsequent RNA samples. Briefly, the RNA was purified and fragmented with divalent cations, followed by synthesis of first-strand cDNA with random hexamer primers and M-MuLV reverse transcriptase. Second-strand cDNA was synthesized with DNA polymerase I and RNaseH, and the rest of the overhangs were converted into blunt ends by exonuclease/polymerase activity. After adenylation of the 3′ ends of DNA fragments, adaptors with hairpin loop structures were attached for hybridization. The library fragments were purified using the AMPure XP system (Beckman Coulter, Brea, CA, USA) to preferentially select cDNA fragments of 370–420 bp in length. Then, PCR products were purified after a polymerase chain reaction (PCR). The library quality was assessed on the Agilent Bioanalyzer 2100 system, and the library preparations were sequenced on an Illumina Novaseq platform. Then, 150 bp paired-end reads were generated.

The reference genome index (http://ftp.ebi.ac.uk/ensemblgenomes/pub/release-51/fungi/fasta/fungi_ascomycota1_collection/neofusicoccum_parvum_ucrnp2_gca_000385595/dna/, accessed on 5 March 2021) was built using HISAT2 v2.0.5 and paired-end clean reads were compared to the reference genome. Fragments per kilobase million (FPKM) were then calculated for each gene based on the length of the gene and the number of reads localized to that gene. Differential expression gene (DEG) analysis of the two conditions/groups was performed using the DESeq2 R package (1.20.0). A P value of 0.05 and an absolute fold change of 1 were set as the thresholds for significant differential expression.

Gene ontology (GO) enrichment analysis of DEGs was implemented by the clusterProfiler R package, correcting gene length bias. The clusterProfiler R package was used to test for statistical enrichment of DEGs in the Kyoto Encyclopedia of Genes and Genomes (KEGG) pathway, to further clarify the advanced functions and connections of biological systems.

2.12. Verification of the Gene Expression Related to Key Pathways

Sixteen genes associated with metabolic processes, cytoskeleton, genetic information processing, and organelles were selected to confirm the RNA-Seq data by quantitative real-time (qRT)-PCR. Total RNA was extracted from fungal mycelia by the TRIzol method, and the concentration of the purified RNA was determined. Then, the first-strand cDNA was synthesized by reverse transcription, based on an RNA PCR Kit (Vazyme Biotech, Nanjing, Jiangsu, China). The amplification program was as follows: one cycle at 95 °C for 5 min and 40 cycles at 95 °C for 10 s and 60 °C for 30 s. Finally, the 2-ΔΔCt method was used to analyze the gene expression data. The primers used for qRT-PCR are listed in Table A1.

2.13. Antifungal Efficacy of DSEO Fumigation In Vivo

The in vivo antifungal efficacy of DSEO was determined according to previous research [11,25]. Cut off the head of the fresh chestnut (the round one with a hard shell) and keep all chestnuts as cross-sectional of the same size as possible. The trimmed chestnuts were disinfected correctly with 75% ethanol and 2% (v/v) sodium hypochlorite solution and left to dry after rinsing with sterile water. A wound with a depth of 2 mm and width of 2 mm was created with a sterile needle, which was inoculated with 10 μL of *N. parvum* mycelial suspension (1 mg/mL), and then left to air-dry. The inoculated fruits were arranged in moistened sealed containers, with 9 fruits per treatment. Filter paper discs were pasted on the bottom of the container with a volume of 600 mL, and DSEO was added to filter paper discs to obtain container volumes of 0.2, 0.4, and 0.8 μL/mL. The containers were sealed and stored at 28 ± 2 °C. The lesion diameter (Mycelia length) was measured by adsorption onto the activated carbon to visualize the mycelium after 3 days.

2.14. The Effect of DSEO Emulsion on the Storage Period of Chestnut

The DSEO emulsion was formulated by mixing the oil and water phases with emulsifiers. DSEO was used as the oil phase, the emulsifiers were 64% Span 80 and 36% Tween 80, and the aqueous phase was deionized water. The mixture was stirred at a speed of 5000 rpm in a magnetic stirrer, and the oil phase was slowly added to the emulsifier. Then, the aqueous phase was added until the solution was completely dissolved and homogeneous. The DSEO concentration was 15% (*v*/*v*), while the emulsifier concentration was 5% (*v*/*v*). A blank emulsion without DSEO was prepared using only the emulsifier and the aqueous phase. Positive control was prepared by mixing natamycin (NM), Tween 80, deionized water with 2% (*v*/*v*) NM, and 1% of Tween 80.

After the DSEO emulsion was stored at room temperature for 30 days, no delamination was observed. The DSEO emulsion was diluted to the required concentration and sprayed on the chestnut, and then the spoilage of the chestnut was recorded every 3 days for a total of 21 days.

2.15. Statistical Analysis

All data are expressed as the means ± standard deviations (SDs). Each treatment consisted of at least three replicates. The results of the in vitro study were analyzed using a one-way analysis of variance (ANOVA) and Duncan's test. Different letters represent significant differences at $p < 0.05$. Statistical significance was set at * $p < 0.05$, ** $p < 0.01$, *** $p < 0.001$.

3. Results

3.1. Yield Rate and Composition of DSEO

The volatile oil extracted from dill seeds was pale yellow with a characteristic aroma, and the yield rate was 1.83 ± 0.16% (*v*/*w*). GC/MS analysis of DSEO identified 10 components representing 99.63% of the total oil. The identified compounds are listed in Table 1. The major components detected in the oil were apiole (39.93%), carvone (23.49%), dihydrocarvone (17.90%), and limonene (16.36%).

Table 1. Chemical composition and content of DSEO.

Peak No.	RI [a]	Compound Name	Content (%)
1	1041	Limonene	16.36
2	1218	Dihydrocarvone	17.90
3	1238	Dihydrocarveol	0.26
4	1246	Carveol	0.17
5	1255	Neodihydrocarveol	0.27
6	1272	Carvone	23.49
7	1549	Myristicin	0.32
8	1576	Elemicin	0.20
9	1652	Apiole	39.93
10	2358	Tetracosanal	0.73
All			99.63

[a] RI is the retention index. It is calculated according to the Van den Dool and Kratz formula using a mixture of C8-C30 n-alkanes.

3.2. In Vitro Antifungal Effect of DSEO

The antifungal effects of different concentrations of DSEO on mycelial growth and fungal biomass of *N. parvum* in vitro are shown in Figure 1. The diameter of mycelia decreased significantly with increased DSEO concentration. The growth of mycelia was completely inhibited at 1 µL/mL DSEO treatment (Figure 1A). DSEO fumigation also has an excellent inhibitory effect on mycelial growth, which can completely inhibit the growth of mycelium at a concentration of 0.2 µL/mL (Figure 1B). Figure 1C shows that, compared to the control group, a significant inhibition rate in *N. parvum* mycelia weight was found at 29.69%, 78.13%, 93.59%, 100.00%, and 100.00%, respectively. These results indicate that

the antifungal effects of DSEO are influenced by both the DSEO concentration and the treatment strategy.

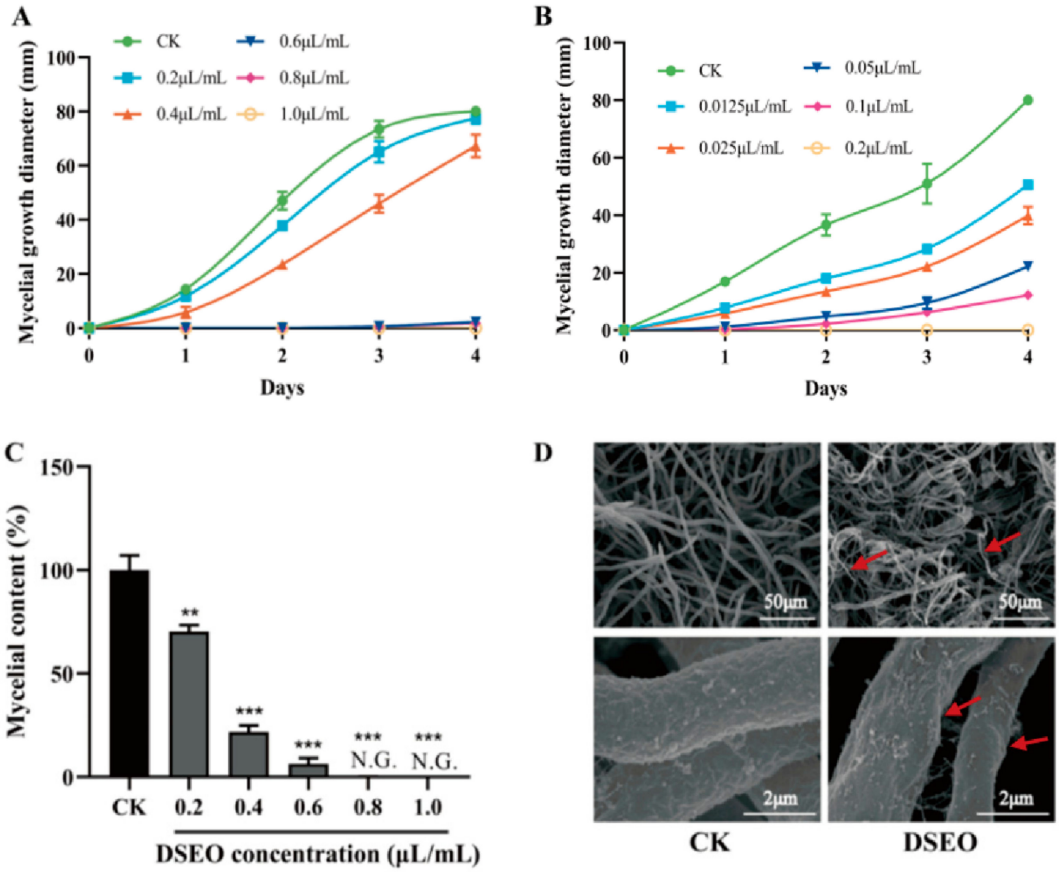

Figure 1. The effect of DSEO on *N. parvum* growth. (**A**) The effect of DSEO on *N. parvum* growth in potato dextrose agar (PDA) medium by direct contact assays; (**B**) The effects of DSEO fumigation on the growth of *N. parvum* in PDA medium by vapor contact assays; (**C**) The effect of DSEO on *N. parvum* growth in potato dextrose broth (PDB) medium, the growth of fungi was shown by the dry weight of mycelium. N.G., No growth. (**D**) Scanning electron microscopy (SEM) images of *N. parvum* with or without DSEO (0.8 μL/mL) treatment. Clear changes were marked with arrows. "CK" represents "control". Statistical significance was set at ** $p < 0.01$, *** $p < 0.001$.

3.3. Effect of DSEO on Mycelial Morphology

The influence of DSEO on the morphology of *N. parvum* was examined using SEM (Figure 1D). The mycelium of the control group had a regular surface morphology, uniform thickness, and smooth cylindrical structure. The mycelia of *N. parvum* treated with DSEO at a concentration of 0.8 μL/mL appeared as multiple folds on the surface, the mycelia were sunken and shriveled, fungal contents leaked, and the thickness of the mycelia was uneven.

3.4. Effect of DSEO on Cell Wall Integrity

Cell wall integrity is critical for fungal growth, an important target for antifungal drugs. The cell wall properties of DSEO-exposed *N. parvum* were examined using the chitin-specific fluorescence dye CFW to analyze the effect of DSEO on the cell wall [26]. As shown in Figure 2A, the mycelia in the control group showed typical blue fluorescence, indicating normal chitin distribution. The mycelia in the DSEO groups showed visibly weaker fluorescence than the control group after 3 h of incubation, indicating that the chitin content was reduced and the cell wall was destroyed. With increasing DSEO concentration, the fluorescence intensity decreased.

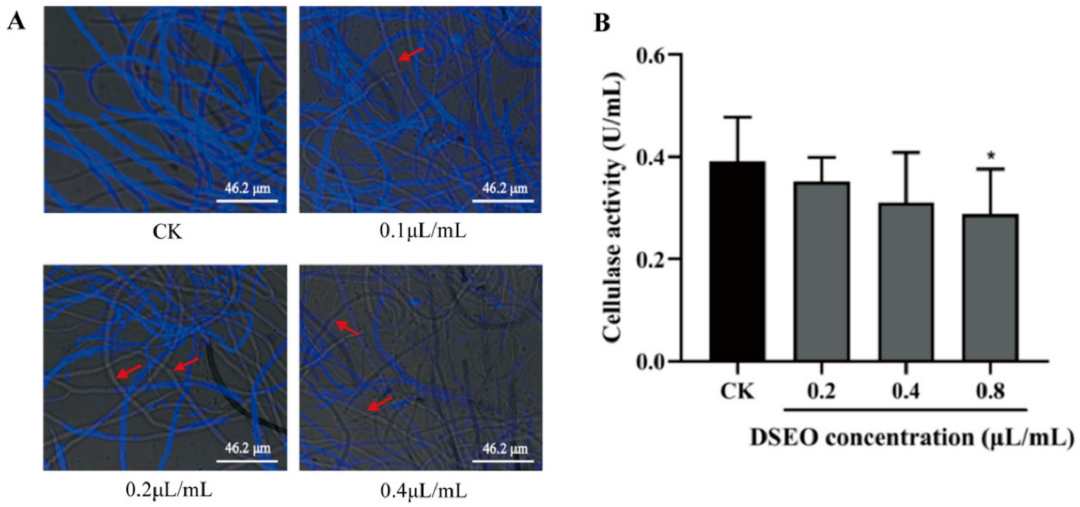

Figure 2. The effects of DSEO on the cell wall of *N. parvum*. (**A**) Merged images under confocal laser scanning microscopy (CLSM) white light and fluorescence after staining with calcium fluorescent white (CFW); Clear changes were marked with arrows. (**B**) The effect of DSEO on the cellulase activity of *N. parvum*. "CK" represents "control". Statistical significance was set at * $p < 0.05$.

To further prove the damage to the fungal cell wall, we measured the activity of cellulase, a cell wall-degrading enzyme [27]. The effect of DSEO on cellulase activity is shown in Figure 2B. Compared with the control group, the cellulase activity did not change significantly when the mycelia were exposed to DSEO at 0.2 μL/mL or 0.4 μL/mL. The cellulase activity decreased significantly when the mycelia were exposed to DSEO at 0.8 μL/mL.

3.5. Effect of DSEO on Plasma Membrane Integrity

The cells were first stained with Evans blue to investigate whether there was a disruption of cell membrane integrity upon exposure to DSEO. As indicated in Figure 3A, when the mycelia were treated with DSEO at a concentration of 0.1 μL/mL, the mycelia were stained blue under a light microscope, suggesting that the cell membranes were compromised after 3 h of treatment with DSEO. With increasing DSEO concentration, the blue color increased significantly, indicating that the plasma membrane was compromised to a greater extent.

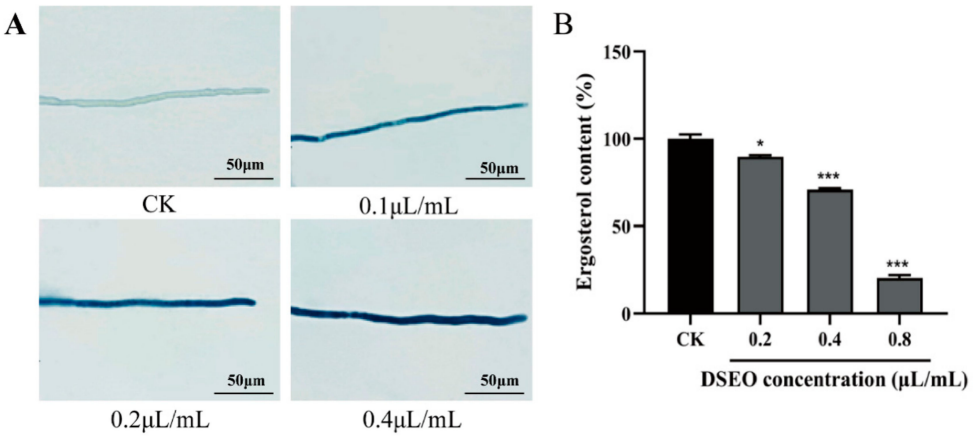

Figure 3. The effects of DSEO on the plasma membrane of *N. parvum*. (**A**) Mycelia were observed under the microscope after staining with Evans blue; (**B**) The effect of DSEO on the content of ergosterol of *N. parvum* after incubation at different concentrations of DSEO for 3 h. "CK" represents "control". Statistical significance was set at * $p < 0.05$, *** $p < 0.001$.

The ergosterol content of *N. parvum* cell membranes was significantly reduced after exposure to DSEO. The inhibition rates of ergosterol biosynthesis in *N. parvum* treated with 0.2 μL/mL, 0.4 μL/mL, and 0.8 μL/mL DSEO were 13.54%, 28.39%, and 71.33%, respectively (Figure 3B).

3.6. Effect of DSEO on the Oxidative Stress Response of N. parvum

As shown in Figure 4A, DSEO induced a pronounced accumulation of TBARS in *N. parvum* at concentrations of 0.2 μL/mL, 0.4 μL/mL, and 0.8 μL/mL, which were 1.50, 2.06, and 2.82 times higher than those in the control group. The results indicated that DSEO could disrupt the fungal cell by oxidative damage.

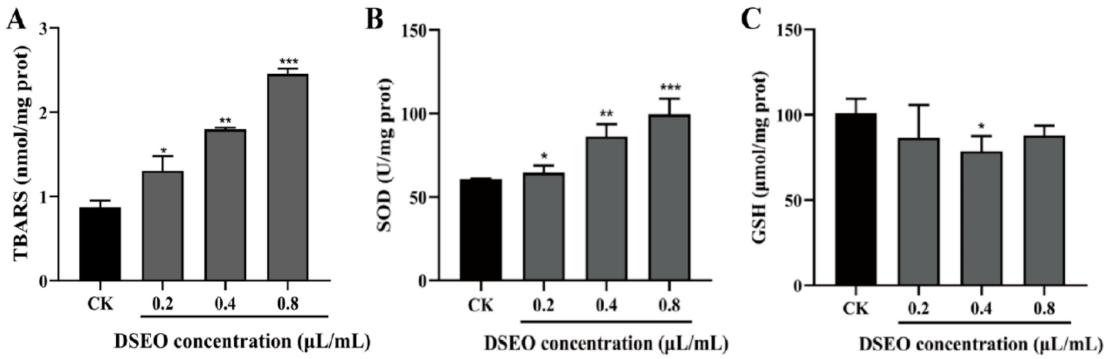

Figure 4. The effects of DSEO on oxidative stress indicators of *N. parvum*, (**A**) MDA levels, (**B**) SOD levels, and (**C**) GSH levels. "CK" represents "control". Statistical significance was set at * $p < 0.05$, ** $p < 0.01$, *** $p < 0.001$.

DSEO exhibited significant enhancement of the cellular antioxidant enzyme SOD, compared to the control. In the control group, the cellular level of SOD was 59.90 units/mg of protein. In contrast, at 0.4 μL/mL and 0.8 μL/mL DSEO treatment, the levels were 86.07 and 98.85 units/mg protein, respectively (Figure 4B).

GSH (γ-glutanylcysteinylglycine) is a tripeptide molecule participating in the nonenzymatic second line of cellular defense and playing an important role in quenching oxyradicals detoxifying xenobiotics. The level of GSH in *N. parvum* decreased after DSEO exposure, and the inhibition rates of DSEO at 0.2 μL/mL and 0.4 μL/mL were 14.21% and 21.99%, respectively. With increasing DSEO concentration, the level of GSH gradually recovered, and the highest concentration of DSEO (0.8 μL/mL) restored the GSH level to 87.19% of the GSH level of the blank group (Figure 4C).

3.7. Transcriptomic Analysis of N. parvum under DSEO Treatment

In this study, 12 samples of *N. parvum* were sequenced by using RNA-seq technology. The principal component analysis (PCA) of variation of the four groups is shown in Figure 5D. Table A2 briefly summarizes the sequencing data information for each sample. A total of 549,876,900 raw reads were preprocessed to obtain 525,036,788 clean reads. High-quality clean data were used to perform subsequent analyses. The Q30 levels were over 92.81%, and the average genome mapping ratio was 94.38%, indicating that the accuracy of the Illumina RNA-Seq data used in the following analysis was reliable.

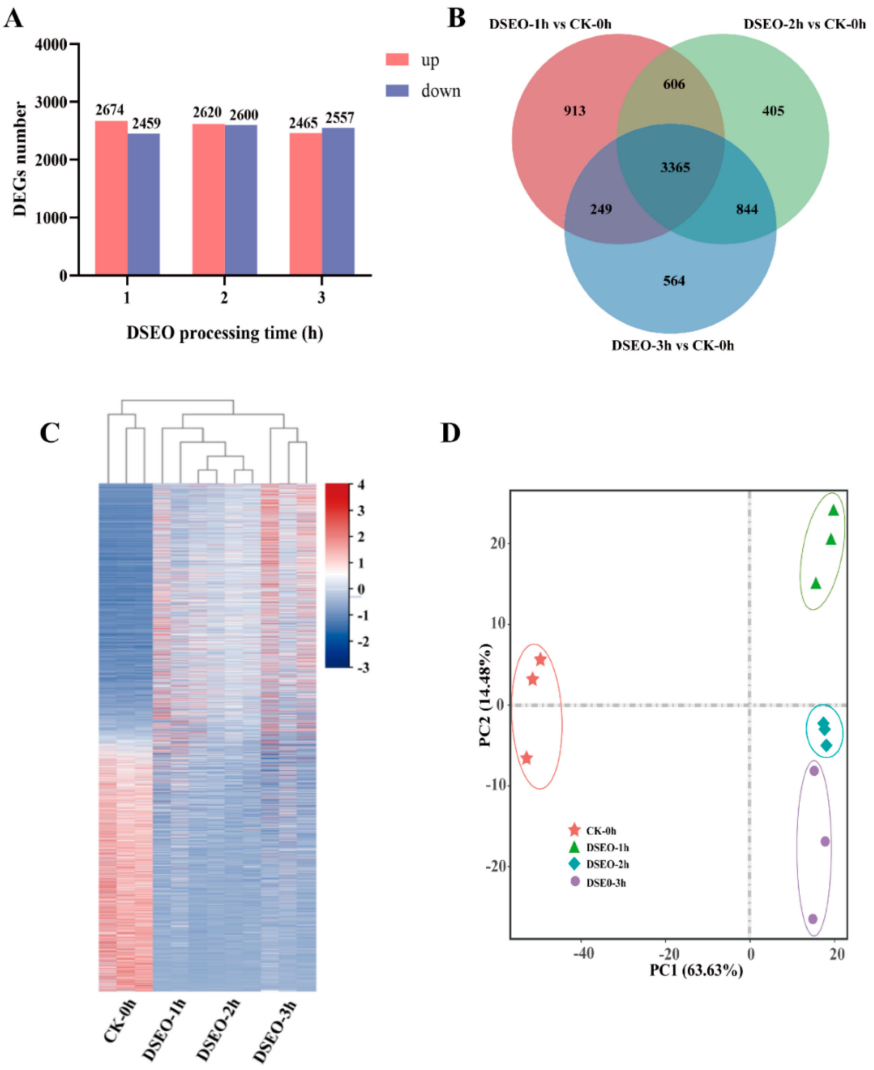

Figure 5. Distribution of DEGs in DSEO-treated and control *N. parvum*. (**A**) Histogram showing the number of DEGs in *N. parvum* after different treatments. (**B**) Venn diagram showing the overlap of DEGs from the 1 h, 2 h, and 3 h datasets. (**C**) Heatmap of DEGs in *N. parvum* before and after DSEO treatment. Each row represents the expression pattern of one gene, and each column corresponds to one sample. (**D**) Principal component analysis (PCA) of transcriptomics data. (n = 3). "CK" represents "control".

Compared with the control group, 5133, 5220, and 5022 genes were found to have changed abundantly after 1 h, 2 h, and 3 h of incubation in the DSEO-treated group (Figure 5A). Based on gene expression analysis, we used Venn diagrams to describe the DEG distribution among several groups (Figure 5B). The overlapping part of the three circles comprised 3365 DEGs. The number of DEGs in DSEO—1 h was the highest, compared with the control group. For a global view of the gene expression profile after exposure to DSEO at different times, a heatmap representing the transcription levels of all DEGs between the four groups was clustered and is shown in Figure 5C; DSEO—1 h and DSEO—2 h clustered into one group, indicating that they have the most similar effects on *N. parvum*. Compared with the control group, the DSEO—1 h group had the most significant number of DEGs, while the DSEO—3 h group had the most significant changes.

All identified DEGs were annotated by gene ontology (GO) analysis and divided into distinct subgroups (Figure 6). GO analysis of DEGs at three treatment timing indicated that the most significant biological process (BP) enrichments were replication, transcription, translation, and lipid, DNA metabolic process. The most significant cellular component

(CC) enrichments occurred in the cytoplasm, intracellular organelle, and cytoskeleton, while molecular function (MF) enrichments occurred in binding and catalytic activity.

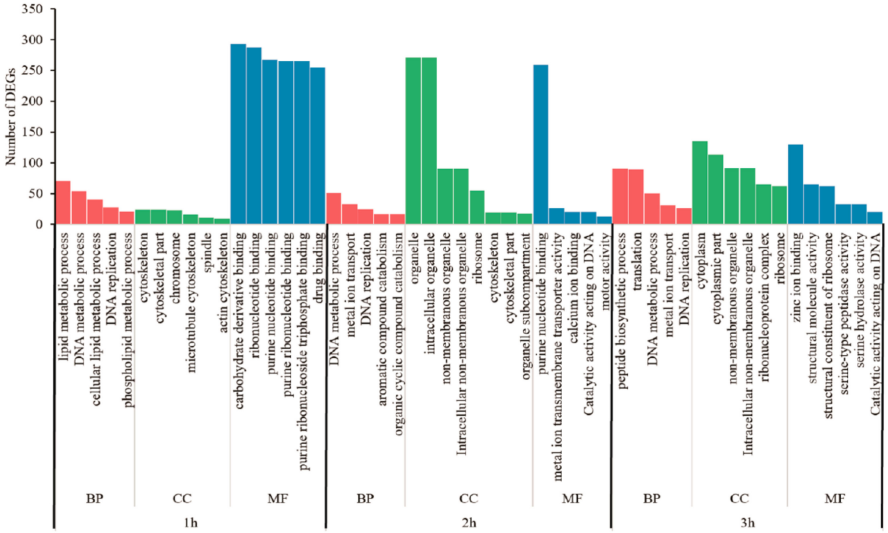

Figure 6. Gene ontology (GO) categorization of DEGs in *N. parvum* after DSEO treatment. GO analysis was performed for three main categories: biological process (BP), cellular component (CC), and molecular function (MF).

Specific biological functions usually result from multiple genes interacting with each other. Based on the Kyoto Encyclopedia of Genes and Genomes (KEGG) pathway database, we aligned the identified DEGs to specific biochemical pathways and outcomes to generate a scatter plot for the top 20 KEGG enrichment results (Figure 7). Pathway classification revealed that most DEGs involved metabolism (such as amino acids, sugars, and lipids) and genetic information processing (such as replication, repair, and recombination). The expression patterns of DEGs were similar at 2 h and 3 h of DSEO treatment. With increasing culture time, the effects of DSEO on the expression of genes involved in the ribosome, secondary metabolite metabolism, and amino acid metabolism were significantly increased.

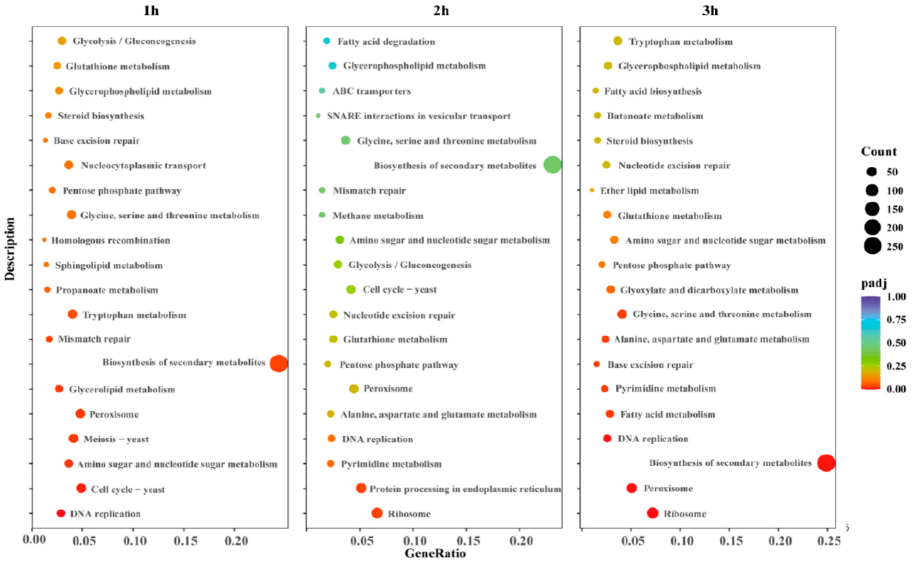

Figure 7. The pathway enrichment statistics of DEGs in *N. parvum* under DSEO stress after 1 h, 2 h, and 3 h of culturing. Gene ratio represents DEGs numbers to all gene numbers annotated in this pathway term. A higher value of the gene ratio means greater intensiveness; padj is a corrected *p*-value ranging from 0 to 1; a lesser *p*-value means greater intensiveness.

3.8. qRT-PCR Validation of Selected DEGs

To verify the reliability of the transcriptome analysis, 16 genes (8 up- and 8 down-regulated) were selected to validate the RNA-seq data by qRT-PCR. As shown in Figure 8, the fold changes in selected DEGs measured by qRT-PCR and RNA-Seq were not precisely consistent. However, they share similar expression profiles, which shows high correlation between RNA-Seq data and transcript abundance detected by qRT-PCR.

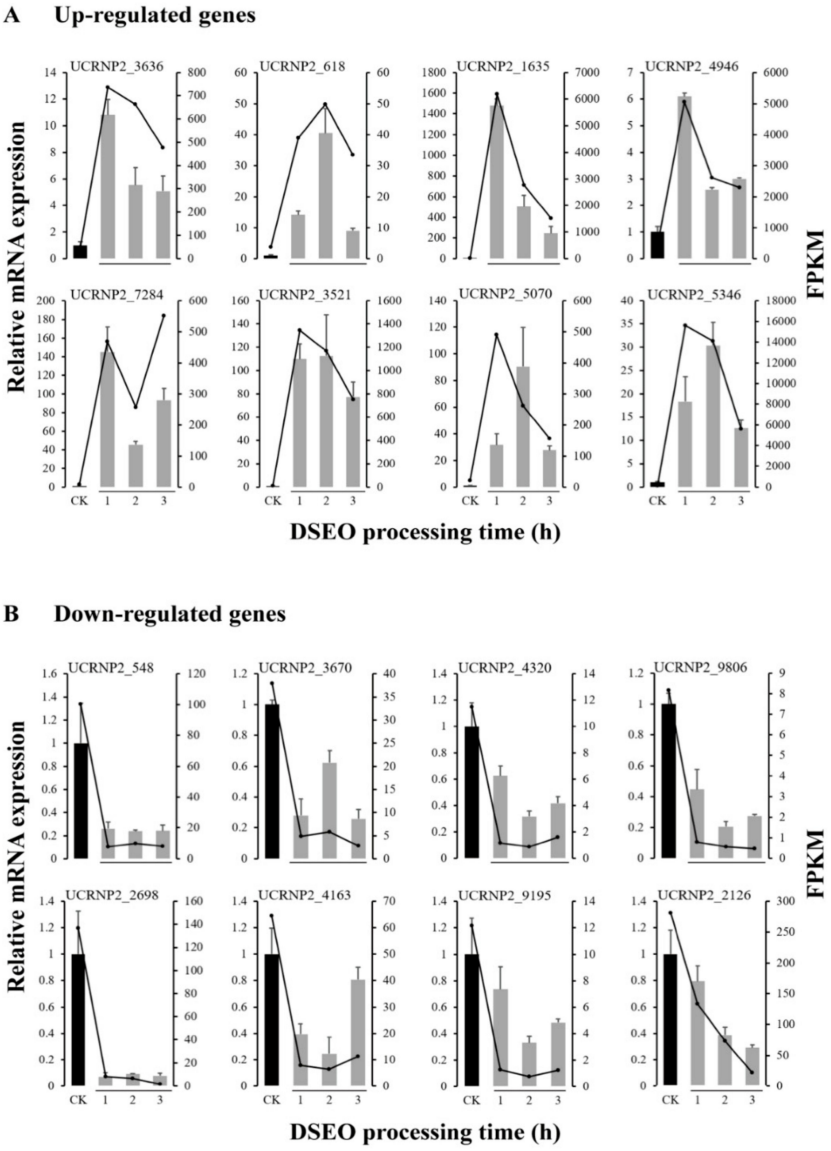

Figure 8. Validation of RNA-Seq data using qRT-PCR data of 16 selected DEGs (8 up- (**A**) and 8 downregulated (**B**)). The central index axis represents relative mRNA expression, and the secondary axis represents the FPKM of genes in transcriptomics. "CK" represents "control".

3.9. Antifungal Efficacy of DSEO Fumigation In Vivo

DSEO has low toxicity and residue advantages, but DSEO has a strong flavor. To avoid affecting the taste of the food, we used the fumigation method to study the antifungal activity of DSEO in vivo. Figure 9 shows the visualized evidence that DSEO could significantly suppress fungal contamination in chestnuts after 3 days of DSEO incubation. With increasing concentrations of DSEO, the protective effect was enhanced. DSEO at a concentration of 0.4 μL/mL significantly inhibited the growth of *N. parvum* in Chinese chestnuts. In comparison, DSEO at a concentration of 0.8 μL/mL almost completely inhibited the growth of *N. parvum* in Chinese chestnuts, ascribed to the gas diffusion capacity of DSEO.

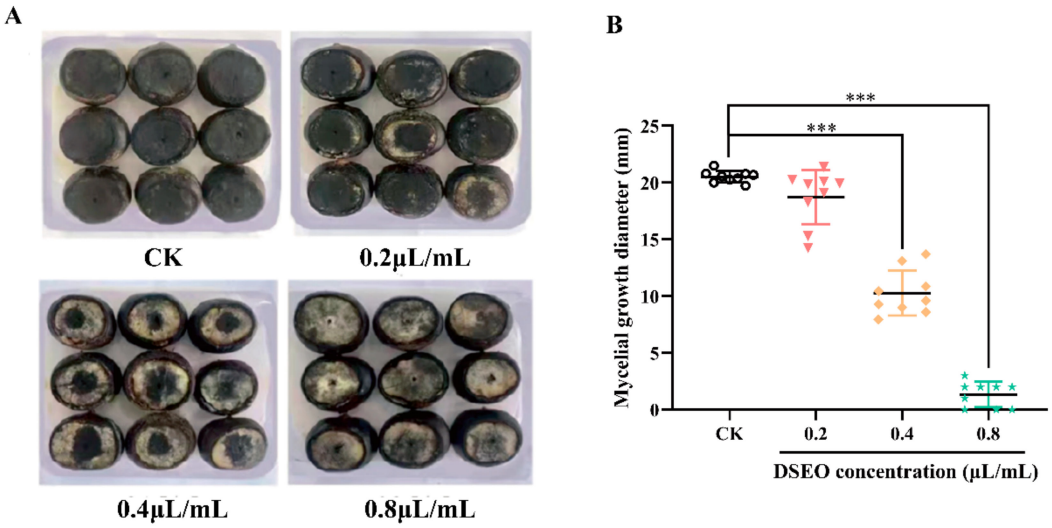

Figure 9. In vivo fumigation antifungal activity of DSEO on the growth of *N. parvum*. (**A**) Representative photos of chestnut samples with or without DSEO treatment during 3 days of incubation and the mycelium length were observed by using the adsorption of activated carbon; (**B**) The effect of DSEO on the growth length of mycelium, n = 9. "CK" represents "control". Statistical significance was set at *** $p < 0.001$.

3.10. DSEO Emulsion Extends the Storage Term of Chestnuts

Although DSEO fumigation can inhibit the growth of pathogens of rot disease in a short time, long-term storage of chestnuts is still a problem and has not yet been solved due to the high volatility of DSEO. To achieve the purpose of long-term storage of chestnut, a DSEO emulsion was employed to prolong the action time of essential oil and improve its bioavailability. The decay rate of chestnuts was expressed by chestnut number and chestnut weight. As shown in Figure 10, both DSEO emulsion concentrations reduced the chestnut decay rate. In the early stage of chestnut storage, the anticorruption effect of the 7.5 μL/mL DSEO emulsion was higher than the anticorruption effect of the 1.5 μL/mL DSEO emulsion, and this significance gradually disappeared with the extension of storage time. Moreover, the DSEO emulsion's effect on prolonging the chestnut storage life is much better than the effect of NM. Therefore, we can choose the concentration of the DSEO emulsion according to the storage time of the Chinese chestnut.

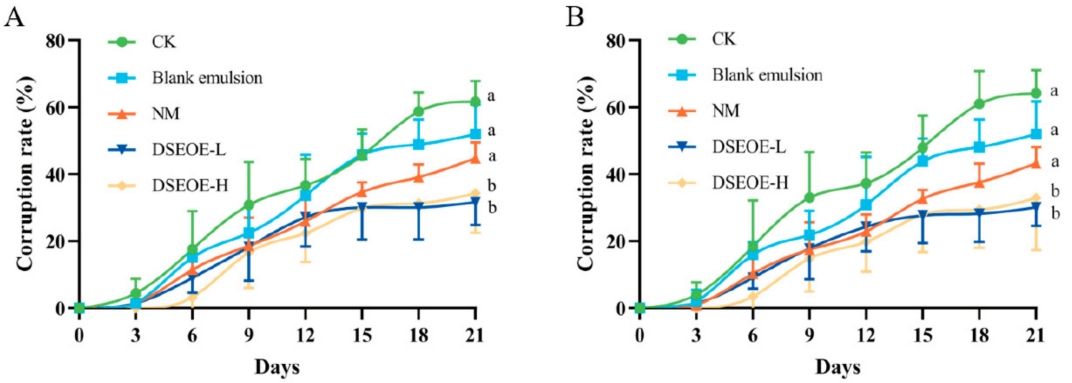

Figure 10. The effect of DSEO emulsion on the storage period of chestnut. (**A**) The number of spoiled chestnuts calculates the spoilage rate of chestnuts; (**B**) The weight of spoiled chestnuts calculates the spoilage rate of chestnuts. NME, 200 μg/mL NM emulsion; DSEOE-L, 1.5 μL/mL DSEO emulsion; DSEOE-H, 7.5 μL/mL DSEO emulsion. Different letters (a and b) indicate a significant difference ($p < 0.05$). "CK" represents "control".

4. Discussion

There has been a growing need for effective and eco-friendly agents to control fungal contamination in food, given the health threat from synthetic chemical fungicides. Essential oil, a natural product from aromatic medicinal plants, was reported to possess antibacterial, antifungal, antioxidant, and anti-inflammatory activities. DSEO is a botanical fungicide in food with broad-spectrum antifungal activity inhibiting pathogens' growth [28,29]. The content of DSEO components varies with geographical conditions, varieties, cultivation patterns, harvest time, extraction methods, etc. [29]. Previous research demonstrated that the main components of DSEO were carvone (41.5%), limonene (32%), and apiole (16.79%), three major compounds [29]. Another study showed that DSEO was primarily composed of carvone (40.36%), limonene (19.31%), and apiole (17.50%) [30]. The main components of our DSEO are apiole (39.93%), carvone (23.49%), dihydrocarvone (17.90%), and limonene (16.36%). Thus, apiole, carvone, and limonene are common major components in the DSEO.

Our study found that the antifungal effects of DSEO against *N. parvum* in vitro could be influenced by the treatment strategy, wherein the growth inhibitory effects of DSEO in gas diffusion were higher than those of liquid culture or that of solid diffusion-induced growth inhibition. In this regard, we investigated the in vivo inhibitory activity of DSEO against *N. parvum* by the fumigation method. Our results showed that DSEO fumigation had a strong protective effect on chestnut storage, which also met the original sensory requirements of foods benefiting from the volatility of DSEO.

There are currently no available reports on the antifungal mechanism of the action of DSEO on *N. parvum*. Our SEM results showed that DSEO treatment resulted in the collapse of the mycelial structure and apparent deformation, indicating loss of cytoplasm and damage to organelles. The fungal cell wall is vital in maintaining cells' inherent morphology and integrity, supporting normal cell metabolism, ion exchange, and osmotic pressure [26]. The experimental data obtained in this work revealed that DSEO treatment significantly reduced the chitin content of the fungal cell wall. This result is consistent with previous studies showing that DSEO exerts antifungal activity by disrupting the cell wall [6,21,31].

In the process of phytopathogenic fungi infecting the host, the pathogenic fungi secrete cellulase to degrade the cell wall of the host plant, which is conducive to the invasion and spread of the pathogenic fungi [20]. Under DSEO treatment, the content of extracellular cellulase in *N. parvum* decreased, and the ability to infect the host was also reduced accordingly. Evans blue staining was employed to investigate whether DSEO affects plasma membrane integrity. Our results showed that the permeability of the cell membrane was compromised by DSEO treatment. Ergosterol is an important component of fungal cell membrane, which can maintain the fluidity and bioregulation of cell membrane [32]. This is also illustrated by the inhibition of ergosterol synthesis by DSEO. Multiple studies have reported that botanical fungicides exert antifungal effects by lowering the membrane ergosterol content [31]. Two major inhibitory mechanisms were explained; one is to disrupt the biosynthesis of ergosterol, and the other is to damage the cell membrane of eukaryotic cells by linking sterols, causing membrane perforation and rupture [19]. Therefore, we reasoned that DSEO might disrupt the cell membrane of eukaryotic cells by linking sterols, affecting its integrity, and, consequently, resulting in macromolecules leakage, thus, we assume that the cell membrane is a target of DSEO against *N. parvum*. Interestingly, similar results have been observed in antifungal studies of other essential oils [16]. Based on their lipophilic character, Eos can penetrate the cell wall through passive diffusion and further destroy the cell membrane [16]. The release of intracellular components leads to cell shrinkage, physiological dysregulation, and even cell death. Blue staining was observed in fungal cells treated with DSEO, confirming cell death [33].

This paper investigated the effect of different concentrations of DSEO on the antioxidant system of fungi. TBARS mainly refers to malondialdehyde (MDA), and MDA is an indicator of cell injury that is generated after exposure to reactive oxygen species (ROS)

and is one of the most important biomarkers of lipid peroxidation [34]. The results showed that TBARS levels were significantly increased after DSEO treatment, indicating that DSEO could damage fungal cells through oxidative damage. In addition, antioxidant systems, such as defense-related antioxidant enzymes, might be activated [35]. Our study found that SOD activity in fungi was elevated to dose-dependent after exposure to DSEO, indicating that DSEO activated the antioxidant enzymes of *N. parvum*. The elevation in SOD activity may be an adaptive response that counteracts some of the negative effects of elevated TBARS in DSEO-exposed *N. parvum* [36]. In addition, a decrease in GSH levels was recorded for *N. parvum* exposed to DSEO. Similar supportive observations have been reported earlier in some studies. The reduction in GSH may cause redox imbalance and impair cell function [36,37].

To better understand the interaction between DSEO and *N. parvum*, RNA-seq methods were used to detect DSEO-induced transcriptome changes in *N. parvum*. Transcriptomic analysis revealed that DSEO affects a wide range of cytoskeleton-related genes. Actin forms filaments ("F- actin" or microfilaments) that are the skeleton fibers in eukaryotic cells, which participate in muscle contraction, deformation, and cytoplasmic separation [38]. The cytoskeleton participates in the formation and division of the cell wall and is a part of the cell wall. At the same time, it is also necessary to maintain cell morphology, material exchange, transport, and cell division. This may explain the cell wall changes observed after the DSEO treatment of *N. parvum*. In earlier reports, the cell membrane was identified as an important target for DSEO to exert its antifungal activity [31,39]. After DSEO treatment, the expression levels of DEGs in metabolic pathways related to cell membrane homeostases, such as phospholipid metabolism and lipid metabolism, were significantly changed. At the same time, with increasing DSEO treatment time, the DEGs regulating the cytoplasm and organelles were downregulated considerably, which supported the previous conclusion that DSEO destroyed the cell wall and cell membrane structure and caused the fungal mycelium to collapse and shrink [21,28]. Most fungi's DEGs related to the ribosome and amino acid metabolism were downregulated. Ribosomes are the site of protein synthesis, and amino acid metabolism mainly synthesizes proteins unique to the body [40]. Therefore, the inhibition of protein biosynthesis may partially explain the antifungal activity of DSEO against fungal pathogens.

5. Conclusions

This study investigated the in vitro antifungal effect of DSEO on *N. parvum*. It explored its mode of action while evaluating its potential as a natural preservative in chestnut storage in vivo. Our results showed that DSEO exhibited solid antifungal activity via gas diffusion and was well applied to food storage. In addition, DSEO can inhibit fungal growth and activity by disrupting the cell wall (cytoskeleton) and cell membrane integrity and inducing intracellular redox imbalance and protein biosynthesis. Most importantly, its high antifungal activity against chestnut samples during storage demonstrates that DSEO may be a promising economic antifungal agent in practice.

Author Contributions: Data curation, T.-T.L., L.-J.G., G.Z., W.-R.D. and Y.C.; Formal analysis, T.-T.L.; Funding acquisition, Y.-X.C.; Methodology, Q.C.; Project administration, Y.-X.C.; Resources, H.Z.; Software, T.-T.L.; Supervision, Q.C. and Y.-X.C.; Writing—original draft, T.-T.L.; Writing—review and editing, H.Z. and Q.C. All authors have read and agreed to the published version of the manuscript.

Funding: This work was supported by the National Natural Science Foundation of China (82104536), Hubei Provincial Natural Science Foundation of China (2020CFB197), Collaborative Grant-in-Aid of the HBUT National "111" Center for Cellular Regulation and Molecular Pharmaceutics (XBTK-2020003, XBTK-2022009), Open Grant from Xinjiang Production & Construction Corps Key Laboratory of Protection and Utilization of Biological Resources in Tarim Basin (BRZD2002), and Doctoral Start-up Foundation of Hubei University of Technology (BSQD2020034, BSQD2020040).

Acknowledgments: We thank Zhi-Jie Liu from the Hubei University of Technology for the GC-MS experiment.

Conflicts of Interest: The authors declared that there are no conflict of interest.

Appendix A

Table A1. Primers used for qRT-PCR.

Gene Symbol	Gene Description	Forward Primer	Reverse Primer
UCRNP2_4935 (actin)	Internal reference gene	GGATGTGCAGGTCATCACAC	GACCACCGAGAAGAGCAAAG
UCRNP2_3636	phospholipid metabolic process	GATGCGGGAGTAGCCTGAC	CCCCAACCAAATCGGTAAGC
UCRNP2_7284	lipid metabolic process	AACTGGGATTAGCGGAAGCC	GACCTGATCAGCGAGCCTAC
UCRNP2_618	DNA metabolic process	GGAAGAGGGGCTGCTTTCTT	GTCCGGATTTGGTGGTCCAT
UCRNP2_3521	DNA binding	GGGGTCAATGTGGTCGAAGT	CCGAGAGGCCCTTTCAAACT
UCRNP2_1635	purine ribonucleotide binding	TCGACCGTCTCCTCTTCCTT	ACCGTTGCGTTCGAAGTAGT
UCRNP2_5070	cell cycle-yeast; cytoskeleton	ATGGCTACACCTCATCCACC	CATGAAGGTCGCCTCATTGTC
UCRNP2_4946	ribosome	AGAAGCGCAAGTCAGCTCAT	CAGAGTCACCTGAGAAGGCG
UCRNP2_5346	hypothetical protein	TCCTCCATCCGCTCTTCGTA	GGCGTTTCCGAGAACAACAC
UCRNP2_548	Amino acid and sugar metabolism	TGGTGGTTTGGAACAGCTTC	ATTGACGCCGGCACATCA
UCRNP2_2698	Fatty acid metabolism	GGTCTTGTCCTGGACTTCGG	CTTCGGCTCTAAGCTCCTCG
UCRNP2_3670	cytoskeleton (actin cytoskeleton)	TGGGGGATTACCAGATTGCG	TCCCACAGGTACACGCTAGA
UCRNP2_4163	cytoskeleton (cytoskeleton part)	GGATATCGCAGGGATGGCAA	GGTACGTCAGGCACTGTGAA
UCRNP2_4320	cytoskeleton	AAAACTTGCCGAGGAGAGGG	ATCGTTATCTCTGCCTGCCG
UCRNP2_9195	organelle	ATGGACTTGGACGCCAACAT	CGACCCAATCGGTCAAGCTA
UCRNP2_9806	non-membrane-bounded organelle	GTGGCTGACGAGGAGGAAAA	GTACTCCTCGAAGCCGATGG
UCRNP2_2126	structural constituent of ribosome	GACCAAGTTCAAGGTCCGCT	CCCATGAGTGTCGTGAGAGG

Table A2. Summary of RNA-seq reads in CK-0h and treatments (DSEO—1 h, DSEO—2 h, DSEO—3 h) groups of *N. parvum*.

Sample	Base Number	Clean Reads	Q30 (%)	GC Content (%)	Mapped Reads	Mapped Ratio (%)
CK-0h-1	46714618	45152836	95.04	59.85	42847419	94.89
CK-0h-2	47740962	45556208	92.81	59.4	42973482	94.33
CK-0h-3	46182706	44575174	94.94	59.8	42355868	95.02
DSE0-1h-1	46699708	45752188	92.55	60.11	42753528	93.45
DSE0-1h-2	46274846	42891208	93.24	60.22	40365528	94.11
DSE0-1h-3	41420784	38231250	93.62	60.41	36136015	94.52
DSE0-2h-1	44093534	41476198	93.43	59.82	38946635	93.90
DSE0-2h-2	44771022	41943828	93.31	59.79	39277988	93.64
DSE0-2h-3	45907572	43027896	93.46	60.39	40713819	94.62
DSE0-3h-1	42078438	39608058	93.36	60.42	37505962	94.69
DSE0-3h-2	48817802	47684086	95.13	59.82	44991433	94.35
DSE0-3h-3	46233786	45365574	95.03	59.51	43080355	94.96

References

1. Li, Q.; Shi, X.; Zhao, Q.; Cui, Y.; Ouyang, J.; Xu, F. Effect of cooking methods on nutritional quality and volatile compounds of Chinese chestnut (*Castanea mollissima* Blume). *Food Chem.* **2016**, *201*, 80–86. [CrossRef] [PubMed]
2. LaBonte, N.R.; Zhao, P.; Woeste, K. Signatures of selection in the genomes of Chinese chestnut (*Castanea mollissima* Blume): The roots of nut tree domestication. *Front. Plant Sci.* **2018**, *9*, 810. [CrossRef] [PubMed]
3. Shuttleworth, L.A.; Liew, E.C.Y.; Guest, D.I. Survey of the incidence of chestnut rot in south-eastern Australia. *Australas. Plant Path.* **2013**, *42*, 63–72. [CrossRef]
4. Seddaiu, S.; Mello, A.; Sechi, C.; Cerboneschi, A.; Linaldeddu, B.T. First Report of Neofusicoccum parvum associated with chestnut nut rot in Italy. *Plant Dis.* **2021**, *105*, 3743. [CrossRef] [PubMed]

5. Waqas, M.; Guarnaccia, V.; Spadaro, D. First report of nut rot caused by *Neofusicoccum parvum* on hazelnut (*Corylus avellana*) in Italy. *Plant Dis.* **2021**, *106*, 1987. [CrossRef] [PubMed]
6. Swanson, H.A.; Svenning, J.C.; Saxena, A. History as grounds for interdisciplinarity: Promoting sustainable woodlands via an integrative ecological and socio-cultural perspective. *One Earth* **2021**, *4*, 226237. [CrossRef]
7. Chen, Y.; Zeng, H.; Tian, J.; Ban, X.; Ma, B.; Wang, Y. Antifungal mechanism of essential oil from *Anethum graveolens* seeds against Candida albicans. *J. Med. Microbiol.* **2013**, *62*, 1175–1183. [CrossRef] [PubMed]
8. Jana, S.; Shekhawat, G.S. *Anethum graveolens*: An Indian traditional medicinal herb and spice. *Pharmacogn. Rev.* **2010**, *4*, 179–184. [CrossRef]
9. Teneva, D.; Denkova, Z.; Denkova-Kostova, R.; Goranov, B.; Kostov, G.; Slavchev, A.; Degraeve, P. Biological preservation of mayonnaise with Lactobacillus plantarum LBRZ12, dill, and basil essential oils. *Food Chem.* **2021**, *344*, 128707. [CrossRef]
10. Kaur, V.; Kaur, R.; Bhardwaj, U.; Kaur, H. Antifungal potential of dill (*Anethum graveolens* L.) seed essential oil, its extracts and components against phytopathogenic maize fungi. *J. Essent. Oil Bear. Plants* **2021**, *24*, 1333–1348. [CrossRef]
11. Boukaew, S.; Prasertsan, P.; Sattayasamitsathit, S. Evaluation of antifungal activity of essential oils against aflatoxigenic *Aspergillus flavus* and their allelopathic activity from fumigation to protect maize seeds during storage. *Ind. Crops Prod.* **2017**, *97*, 558–566. [CrossRef]
12. Kumar, N.; Khurana, S.M.; Pandey, V.N. Application of clove and dill oils as an alternative of salphos for chickpea food seed storage. *Sci. Rep.* **2021**, *11*, 10390. [CrossRef]
13. Yang, K.; Liu, A.; Hu, A.; Li, J.; Zen, Z.; Liu, Y.; Li, C. Preparation and characterization of cinnamon essential oil nanocapsules and comparison of volatile components and antibacterial ability of cinnamon essential oil before and after encapsulation. *Food Control* **2021**, *123*, 107783. [CrossRef]
14. Xu, D.; Wei, M.; Peng, S.; Mo, H.; Huang, L.; Yao, L.; Hu, L. Cuminaldehyde in cumin essential oils prevents the growth and aflatoxin B1 biosynthesis of *Aspergillus flavus* in peanuts. *Food Control* **2021**, *125*, 107985. [CrossRef]
15. Ju, J.; Xie, Y.; Yu, H.; Guo, Y.; Cheng, Y.; Zhang, R.; Yao, W. Major components in *Lilac* and *Litsea cubeba* essential oils kill *Penicillium roqueforti* through mitochondrial apoptosis pathway. *Ind. Crops Prod.* **2020**, *149*, 112349. [CrossRef]
16. Sun, Q.; Li, J.; Sun, Y.; Chen, Q.; Zhang, L.; Le, T. The antifungal effects of cinnamaldehyde against *Aspergillus niger* and its application in bread preservation. *Food Chem.* **2020**, *317*, 126405. [CrossRef]
17. Jiang, N.; Wang, L.; Jiang, D.; Wang, M.; Liu, H.; Yu, H.; Yao, W. Transcriptomic analysis of inhibition by eugenol of ochratoxin A biosynthesis and growth of *Aspergillus carbonarius*. *Food Control* **2020**, *135*, 108788. [CrossRef]
18. Long, Y.; Huang, W.; Wang, Q.; Yang, G. Green synthesis of garlic oil nanoemulsion using ultrasonication technique and its mechanism of antifungal action against *Penicillium italicum*. *Ultrason. Sonochem.* **2020**, *64*, 104970. [CrossRef]
19. OuYang, Q.; Okwong, R.O.; Chen, Y.; Tao, N. Synergistic activity of cinnamaldehyde and citronellal against green mold in citrus fruit. *Postharvest Biol. Technol.* **2020**, *162*, 111095. [CrossRef]
20. Khaledi, N.; Taheri, P.; Tarighi, S. Antifungal activity of various essential oils against *R hizoctonia solani* and *Macrophomina phaseolina* as major bean pathogens. *J. Appl. Microbiol.* **2015**, *118*, 704–717. [CrossRef]
21. Oliveira, R.C.; Carvajal-Moreno, M.; Mercado-Ruaro, P.; Rojo-Callejas, F.; Correa, B. Essential oils trigger an antifungal and anti-aflatoxigenic effect on *Aspergillus flavus* via the induction of apoptosis-like cell death and gene regulation. *Food Control* **2020**, *110*, 107038. [CrossRef]
22. Hu, Y.; Zhang, J.; Kong, W.; Zhao, G.; Yang, M. Mechanisms of antifungal and anti-aflatoxigenic properties of essential oil derived from turmeric (*Curcuma longa* L.) on *Aspergillus flavus*. *Food Chem.* **2017**, *220*, 1–8. [CrossRef]
23. Kong, J.; Zhang, Y.; Ju, J.; Xie, Y.; Guo, Y.; Cheng, Y.; Yao, W. Antifungal effects of thymol and salicylic acid on cell membrane and mitochondria of *Rhizopus stolonifer* and their application in postharvest preservation of tomatoes. *Food Chem.* **2019**, *285*, 380–388. [CrossRef]
24. Yan, J.; Wu, H.; Shi, F.; Wang, H.; Chen, K.; Feng, J.; Jia, W. Antifungal activity screening for mint and thyme essential oils against *Rhizopus stolonifer* and their application in postharvest preservation of strawberry and peach fruits. *J. Appl. Microbiol.* **2021**, *130*, 1993–2007. [CrossRef]
25. Zhao, Y.; Yang, Y.H.; Ye, M.; Wang, K.B.; Fan, L.M.; Su, F.W. Chemical composition and antifungal activity of essential oil from *Origanum vulgare* against *Botrytis cinerea*. *Food Chem.* **2021**, *365*, 130506. [CrossRef]
26. Xu, T.; Cao, L.; Zeng, J.; Franco, C.M.; Yang, Y.; Hu, X.; Zhu, Y. The antifungal action mode of the rice endophyte Streptomyces hygroscopicus OsiSh-2 as a potential biocontrol agent against the rice blast pathogen. *Pestic. Biochem. Phys.* **2019**, *160*, 58–69. [CrossRef]
27. Xu, T.; Li, Y.; Zeng, X.; Yang, X.; Yang, Y.; Yuan, S.; Zhu, Y. Isolation and evaluation of endophytic Streptomyces endus OsiSh-2 with potential application for biocontrol of rice blast disease. *J. Sci. Food Agric.* **2017**, *97*, 1149–1157. [CrossRef]
28. Tian, J.; Ban, X.; Zeng, H.; He, J.; Chen, Y.; Wang, Y. The mechanism of antifungal action of essential oil from dill (*Anethum graveolens* L.) on *Aspergillus flavus*. *PLoS ONE* **2012**, *7*, e30147. [CrossRef]
29. Ma, B.; Ban, X.; Huang, B.; He, J.; Tian, J.; Zeng, H.; Wang, Y. Interference and mechanism of dill seed essential oil and contribution of carvone and limonene in preventing Sclerotinia rot of rapeseed. *PLoS ONE* **2015**, *10*, 131733. [CrossRef]
30. Li, H.; Zhou, W.; Hu, Y.; Mo, H.; Wang, J.; Hu, L. GC-MS analysis of essential oil from *Anethum graveolens* L (dill) seeds extracted by supercritical carbon dioxide. *Trop. J. Pharm. Res.* **2019**, *18*, 1291–1296. [CrossRef]

31. Wei, J.; Bi, Y.; Xue, H.; Wang, Y.; Zong, Y.; Prusky, D. Antifungal activity of cinnamaldehyde against *Fusarium sambucinum* involves inhibition of ergosterol biosynthesis. *J. Appl. Microbiol.* **2020**, *129*, 256–265. [CrossRef] [PubMed]
32. OuYang, Q.; Tao, N.; Jing, G. Transcriptional profiling analysis of *Penicillium digitatum*, the causal agent of citrus green mold, unravels an inhibited ergosterol biosynthesis pathway in response to citral. *BMC Genom.* **2016**, *17*, 599. [CrossRef] [PubMed]
33. Donadu, M.G.; Peralta-Ruiz, Y.; Usai, D.; Maggio, F.; Molina-Hernandez, J.B.; Rizzo, D.; Chaves-Lopez, C. Colombian essential oil of *Ruta graveolens* against nosocomial antifungal resistant *Candida strains*. *J. Fungi* **2021**, *7*, 383. [CrossRef] [PubMed]
34. Dan, W.; Gao, J.; Li, L.; Xu, Y.; Wang, J.; Dai, J. Cellular and non-target metabolomics approaches to understand the antifungal activity of methylaervine against *Fusarium solani*. *Bioorg Med. Chem. Lett.* **2021**, *43*, 128068. [CrossRef] [PubMed]
35. Hua, C.; Kai, K.; Bi, W.; Shi, W.; Liu, Y.; Zhang, D. Curcumin induces oxidative stress in *Botrytis cinerea*, resulting in a reduction in gray mold decay in kiwifruit. *J. Agric. Food Chem.* **2019**, *67*, 7968–7976. [CrossRef] [PubMed]
36. Kiran, S.; Prakash, B. Toxicity and biochemical efficacy of chemically characterized Rosmarinus officinalis essential oil against *Sitophilus oryzae* and *Oryzaephilus surinamensis*. *Ind. Crops Prod.* **2015**, *74*, 817–823. [CrossRef]
37. Kumar, A.; Kujur, A.; Yadav, A.; Pratap, S.; Prakash, B. Optimization and mechanistic investigations on antifungal and aflatoxin B1 inhibitory potential of nanoencapsulated plant-based bioactive compounds. *Ind. Crops Prod.* **2019**, *131*, 213–223. [CrossRef]
38. Pollard, T.D.; Cooper, J.A. Actin, a central player in cell shape and movement. *Science* **2009**, *326*, 1208–1212. [CrossRef]
39. Chen, Y.; Zeng, H.; Tian, J.; Ban, X.; Ma, B.; Wang, Y. Dill (*Anethum graveolens* L.) seed essential oil induces *Candida albicans* apoptosis in a metacaspase-dependent manner. *Fungal Biol.* **2014**, *118*, 394–401. [CrossRef]
40. Batista-Silva, W.; Heinemann, B.; Rugen, N.; Nunes-Nesi, A.; Araújo, W.L.; Braun, H.P.; Hildebrandt, T.M. The role of amino acid metabolism during abiotic stress release. *Plant Cell Environ.* **2019**, *42*, 1630–1644. [CrossRef]